Journal of Inflammation Research

Dovepress
Taylor & Francis Group

Open Access Full Text Article

ORIGINAL RESEARCH

Qing'e Pills Ameliorates Osteoporosis by Regulating Gut Microbiota and Th17/Treg Balance in Ovariectomized Rats

Fangyu Hao[1,2,*], Mengyu Guo[1,2,*], Yuwei Zhao[1,2], Xingyu Zhu[1,2], Xiaofang Hu[1,2], Weihao Zhu[1,2], Chunmei Mei[1,2], Nong Zhou[3], Kunming Qin[4], Hui Zhu[1,2], Weidong Li[1,2]

[1]School of Pharmacy, Nanjing University of Chinese Medicine, Nanjing, People's Republic of China; [2]Jiangsu Key Laboratory of Chinese Medicine Processing, Engineering Center of State Ministry of Education for Standardization of Chinese Medicine Processing, Nanjing University of Chinese Medicine, Nanjing, People's Republic of China; [3]College of Biology and Food Engineering, Chongqing Three Gorges University, Chongqing, People's Republic of China; [4]School of Pharmacy, Jiangsu Ocean University, Lianyungang, People's Republic of China

*These authors contributed equally to this work

Correspondence: Hui Zhu; Weidong Li, School of Pharmacy, Nanjing University of Chinese Medicine, Nanjing, People's Republic of China, Email zhui_0826@njucm.edu.cn; liweidong0801@163.com

Purpose: Bone metabolism disorders are strongly associated with T helper type 17/regulatory T (Th17/Treg) cell imbalance and inflammatory dysregulation. Qing'e pills (QEP) is a classical prescription for treating osteoporosis with both safety and clinical effectiveness. However, the mechanism of its immune action remains unclear.

Methods: QEP components were identified via HPLC. Anti-osteoporotic effects of QEP were assessed through biochemical, micro computed tomography, bone biomechanical and histopathological analyses. Th17/Treg balance and related inflammatory factors were analyzed using flow cytometric, biochemical, immunohistochemical, and quantitative real-time PCR assays. The effects of QEP on gut microbiota and endogenous metabolites were analyzed via 16S rRNA analysis, co-incubation experiments and untargeted metabolomics. Integrative correlations analysis was used to explore the relationships among gut-bone-Th17/Treg balance interactions.

Results: QEP improved bone mineral density and bone biomechanical properties and reduced bone conversion in ovariectomized rats. After treatment, QEP restored intestinal barrier integrity, and reduced serum LPS levels. QEP significantly decreased Th17-related inflammatory cytokines TNF-α, IL-17 levels, reduced the transcription of Th17-related genes RORγt and IL-17A and the percentage of CD4+IL-17A+ Th17 cells in the gut-bone axis, and concurrently restored the anti-inflammatory cytokines levels of TGF-β and IL-10, the expression of Foxp3 and the percentage of CD4+ CD25+ Foxp3+ Treg cells in the gut–bone axis. Notably, QEP improved the disorganization of gut microbiota composition and structure in ovariectomized rats. On genus level, QEP can significantly increase the relative abundance of *Lactobacillus* in vitro and in vivo. Furthermore, gut microbe-derived endogenous metabolites potentially mediating QEP's regulation of Th17/Treg balance in gut-bone axis and anti-osteoporotic effects.

Conclusion: QEP ameliorates osteoporosis by improving the intestinal flora disorders and immune status, and restoring the balance of Th17/Treg in the gut-bone axis, highlighting its clinical potential in the treatment of postmenopausal osteoporosis.

Keywords: Qing'e pills, osteoporosis, Th17/Treg, gut microbes, *Lactobacillus*

Introduction

Osteoporosis is a prevalent systemic bone disorder characterized by reduced bone strength and elevated risk of fracture with reduced quality of life and increased financial burden worldwide. Taking in consideration the effect of the aging of the population,[1] the burden of osteoporosis and fragility fractures is projected to increase dramatically. Therefore, it is crucial to address the treatment and prevention of osteoporosis. Although, the fracture incidence varies substantially across countries, women over 50 years of age have an average risk as high as 50%.[2] As the ovarian degeneration and decreased estrogen secretion can lead to disorganized bone metabolism.[3] Currently, bisphosphonates and hormone

Received: 30 January 2025
Accepted: 16 May 2025
Published: 11 June 2025

Graphical Abstract

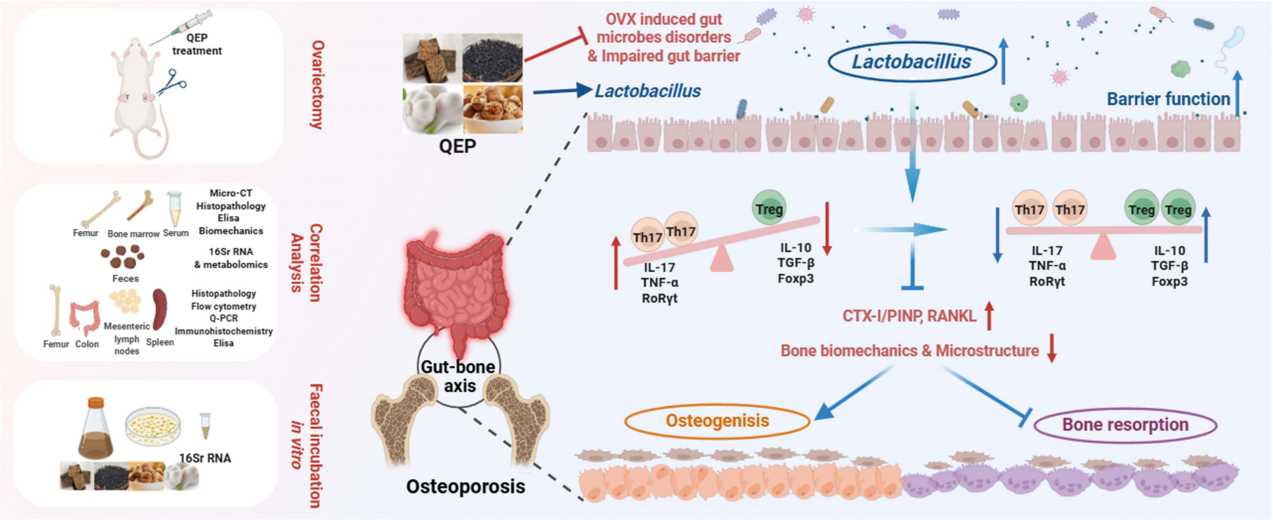

replacement therapy are commonly used to treat postmenopausal osteoporosis (PMOP). However, these therapies are limited by high costs, poor adherence, and adverse reactions after long-term administration. For example, adverse events of bisphosphonates include abdominal pain, dyspepsia, acid regurgitation, musculoskeletal pain, and even osteonecrosis of the jaw.[4–6] Moreover, long-term use of drugs like estrogen and calcitonin might result in an elevated susceptibility to malignancy.[7] Therefore, safe and efficacious novel interventions are needed for the prevention and management of osteoporosis.

The gut microbiome has been shown to have a profound effect on bone quality and overall strength in many clinical studies. Recently, probiotics are being increasingly investigated as cost-effective and low-risk pharmacotherapies for osteoporosis, having been shown to improve bone density by enhancing intestinal epithelial integrity, reducing antigen presentation, and activating intestinal immune cells.[3] Notably, the intestinal barrier, acting as a dwelling and safeguard for the gut microbiota, can be dysfunctional due to sex steroid deficiency in women during menopause, followed by increased circulating lipopolysaccharide (LPS) levels and $CD4^+$ T cell.[8] Notably, in studies on bone immunology, under chronic inflammatory conditions caused by estrogen deficiency, T cell subset distribution is disturbed, T helper type 17/regulatory T (Th17/Treg) cell imbalance and related inflammatory factors have been found to be closely associated with disorders of bone metabolism.[9] In particular, due to estrogen deficiency, the differentiation response of Th17 cells was enhanced, further promoting the secretion of IL-17, RANKL and TNF as well as IFN-γ, which effectively induced osteoclastogenesis. In addition, IL-17 increases the osteoclastogenic activity by stimulating the release of RANKL from all osteoblasts.[10,11] Notably, numerous clinical studies have demonstrated that the gut microbiome exerts a profound influence on bone quantity and strength by regulating metabolites and influencing endocrine and immune pathways. Therefore, the immune pathway serves as an important intersection between bone microbiology and immunology and has significant implications for research on the gut–bone axis.[12,13]

Qing'e pills (QEP), comprised of the *Eucommia ulmoides* Oliv., *Psoralea corylifolia* Linn., *Juglans regia* L., and *Allium sativum* L., is a well-known classical prescription for tonifying the kidneys and strengthening bones clinically.[14] Studies have shown that QEP was continuously administered at normal dose or multiple doses for 3 months without obvious side effects, suggesting the safety and reliability of it in clinical use.[15,16] Notably, QEP has been clinically used to treat the climacteric syndrome, especially perimenopausal osteoporosis, with the estrogen-like properties for directly stimulating the balance between osteoblasts and osteoclasts.[17] Our previous study had shown that QEP can modulate the gut microbiota in ovariectomized (OVX) rat, and the gut microbiota serves as a target for its anti-osteoporotic effect.

Furthermore, OVX rats exhibited damaged ileum and increased serum levels of tumor necrosis factor-α (TNF-α), IL-6, and IL-17.[18] Therefore, further elucidating the underlying mechanism through which QEP exerts its anti-osteoporotic effect via the gut microbiota and immune pathways is imperative. Hence, the novelty of this study lies in uncovering QEP exerts its anti-osteoporotic effect by modulating gut microbiota and improving the inflammatory status, which were mediated by the mechanism involved in regulating Th17/Treg balance and related inflammatory factors in the gut-bone axis.

Materials and Methods

Preparation and Analysis of the QEP and Phytocomponents

Salted *Eucommia ulmoides* (Yunnan, China), salted *Psoralea corylifolia* (Yunnan, China), fried *Juglans regia* (Anhui, China), and steamed *Allium sativum* (Henan, China) were combined in a ratio of 16:8:5:4, respectively. All Chinese herbs of QEP were identified by Professor Jianguo Chao, Department of Chinese Materia Medica Identification, Nanjing University of Chinese Medicine. Voucher specimens were deposited in the pharmacy school of Nanjing University of Chinese Medicine. QEP powder (500 g) was mixed with 5 L of 95% ethanol and refluxed for 2 h. Subsequently, 5 L of pure water was added for an additional 2 h of extraction. Finally, the extract was concentrated to obtain a low-dose concentration of 0.6 g/mL (QEPL) and a high-dose concentration of 3 g/mL (QEPH).

The QEP extract contained 0.027% geniposidic acid, 0.306% psoralenoside, 0.206% isopsoralenoside, 0.214% psoralen, 0.147% isopsoralen, 0.038% isobavachin, 0.114% neobavaisoflavone, 0.047% bavachin, 0.125% bavachalcone, 0.077% isobavachalcone, 0.273% bavachinin, 0.176% corylifol A, 0.058% 4′-*O*-methylbroussochalcone B, and 1.477% bakuchiol. The HPLC chromatogram of the QEP extract is displayed in Figure S1. The HPLC analysis was performed as previously described.[18]

Animals and Drug Administration

Forty female Sprague-Dawley rats (220–260 g) were obtained from the Laboratory Animal Center of Hangzhou Medical College (SCXK [Zhejiang] 2019–0002). The animals were kept under a standard 12/12 h light/dark cycle in a specific pathogen-free environment at a constant temperature of 20–24°C and humidity of 45–60% and fed adaptively for 7 d.

For osteoporosis modeling, the experimental rats were first anesthetized with an intraperitoneal injection of pentobarbital sodium (30 mg/kg; 0.1 mL/100 g), and then the rats were placed in a lateral position for surgery. The ovarian tissue was removed from the back of the rodent body. For the Sham group, only the same weight of adipose tissue was removed. After ovariectomy, the wound of rats was sutured with absorbable sutures, and the rats were given intramuscular injection of penicillin and placed in an incubator until the rats recovered from anesthesia. The rats were randomly divided into four groups of 10 rats each: Sham, OVX, QEPL and QEPH and recovered for 6 weeks after surgery. Subsequently, QEPL and QEPH groups were treated via oral gavage for 6 weeks. Food and water were provided ad libitum during the experimental periods. Referring to the adult recommended dosage of QEP in the 2020 edition of the Chinese Pharmacopoeia, QEP doses were calculated by the body surface area normalization method. The clinical human dosage was converted to equivalent rat doses by multiplying it by 6.3 (the scaling factor between humans and rats) and dividing by 60 kg (the weight of a typical human). Five times the doses of QEPL were selected as the doses of QEPH. Thus, the doses for rats of QEPL and QEPH were, respectively, 3 and 15 $g \cdot kg^{-1} \cdot d^{-1}$. The two other groups received 1 mL of sterile water orally daily. The body weights were measured weekly during treatment.

Biochemical Analysis

Serum stored at −80°C was thawed, and the calcium (Ca) content was quantified using a Ca detection kit (Qiangsheng Biotechnology, Zhejiang, China) and an automated biochemical analyzer. The levels of estradiol, procollagen type I N-terminal propeptide, C-telopeptide of type I collagen, and lipopolysaccharide (LPS) were measured using enzyme-linked immunosorbent assay (ELISA). The tumor necrosis factor-alpha (TNF-α), interleukin (IL)-17, transforming growth factor-beta (TGF-β), IL-10, and LPS levels were assessed in the supernatant of the grounded colon samples, whereas the TNF-α, IL-17, TGF-β, IL-10, and receptor activator for nuclear factor-kappa B ligand levels were assessed in

the bone marrow tissue samples. The ELISAs were performed using ELISA kits (AiFang Biological, Beijing, China) according to the manufacturer's instructions.

Bone Biomechanics

Rat femurs were fixed using an Acumen3 biomechanical tester (MTS Systems, Eden Prairie, MN, USA). The three-point bending method was applied until the femur fractured, and the load-displacement curves of stiffness, ultimate load, and deflection parameters were subsequently plotted.

Bone Histopathology

Femoral tissues were fixed in a 4% paraformaldehyde solution for 1 week and then decalcified in ethylenediaminetetraacetic acid solution for 4 weeks. After embedding in paraffin, sections of 4 μm thickness were prepared and subjected to tartrate-resistant acid phosphatase (TRAP) staining. The subchondral bone adjacent to the cartilage boundary was selected as the observation area.

Additionally, decalcified distal femoral tissues were embedded in paraffin, and sections of 4 μm thickness were prepared. Immunohistochemical staining was performed using anti-Foxp3 (AF14722, AiFang Biological, Changsha, Hunan, China) and anti-RORγt antibodies (AF03308, AiFang Biological).

Bone Microstructure Analysis

The distal femur was fixed and scanned using a micro computed tomography (Micro-CT) instrument (Skyscan 1176, Bruker, Belgium) operated under the following conditions: 65 kV voltage, 385 μA current, 18 μm slice thickness, and 0.24°/r rotation angle. The bone mineral density (BMD), bone volume fraction (BV/TV), trabecular number (Tb.N), trabecular thickness (Tb.Th), trabecular separation (Tb.Sp), and structure model index (SMI) were recorded.

Colonic Histopathology

The colon tissue was fixed using a 4% paraformaldehyde solution and then embedded in paraffin. Subsequently, sections of 4 μm thickness were prepared and stained with hematoxylin and eosin (AiFang Biological). The histopathological analysis included assessments of crypt damage (graded on a scale from 0 to 4), inflammation severity (graded on a scale from 0 to 3), and goblet cell damage (graded on a scale from 0 to 3).

Flow Cytometric Analysis of Th17/Treg in MLN

Approximately 100 mg of MLN tissue was homogenized and centrifuged at 800 rpm for 10 min. Subsequently, the tissue suspension was incubated with a protein transport inhibitor enzyme (S1753, Beyotime, Shanghai, China) at a concentration of 3 μM. Subsequently, APC-anti-mouse-CD4 (213644, Elabscience, Houston, TX, USA), PE-cy5-anti-mouse-CD4 (15–0041-81, eBioscience, San Diego, CA, USA), and APC-anti-mouse-CD25 antibodies (208614, Elabscience) were added to the suspension, and the mixture was incubated in the dark at 37°C for 30 min. Subsequently, a fixative solution (2330512, Invitrogen, Waltham, MA, USA) was added, and the mixture was incubated for another 30 min. The resulting mixture was centrifuged, followed by the addition of a membrane-breaking solution (2330512, Invitrogen). This mixture was incubated and then centrifuged. Finally, PE-anti-mouse IL-17A (212368, Elabscience) or PE anti-mouse forkhead box P3 (Foxp3) antibodies (213511, Elabscience) were used to stain the cells. A flow cytometer (CytoFLEX, Beckman Coulter, Brea, CA, USA) was used to analyze the cell phenotypes.

RNA Extraction and Quantitative Real-Time PCR

RNA was extracted from colonic tissue using the Ultrapure Total RNA Extraction Kit (CW0581S, Kangwei Century Biotechnology Co., Ltd., Beijing, China). A UV absorption method (NanoDrop® ND-2000, Thermo Fisher Scientific, Waltham, MA, USA) was used to determine the concentration and purity of the RNA, after which cDNA was synthesized from the RNA using the HiScript III 1st Strand cDNA Synthesis Kit (+gDNA wiper) (R312-01, Nanjing Nuoweizan, Nanjing, China). qRT-PCR analysis of the synthesized cDNA was performed with the AceQ Universal SYBR qPCR Master Mix (Q511-02, Nanjing Nuoweizan) on a real-time PCR system (ABI 7500, Applied Biosystems, Waltham, MA,

USA). The primers for targeting the *Foxp3*, RAR-related orphan receptor gamma t (*RORγt*), and *IL-17A* genes are listed in Table S1.

16S rRNA Sequencing and Analysis

The total genomic DNA of the microbial communities was extracted using the E.Z.N.A.® Soil DNA Kit according to the manufacturer's instructions. The resulting DNA was used as a template for subsequent analyses. PCR targeting the V3–V4 variable region of the 16S rRNA gene was performed using the following primers: 338F (5′-ACTCCTACGGGAGGCAGCAG-3′) upstream and 806R (5′-GGACTACHVGGGTWTCTAAT-3′) downstream. Sequencing was performed using an Illumina MiSeq PE300/NovaSeq PE250 platform.

UPLC-Q/TOF-MS for Fecal Metabolomics

The fecal sample from QEP-treated rats was homogenized in methanol and centrifuged (13,000 rpm, 10 min). The resulting mixture was filtered through a 0.22 μm filter and centrifuged again (13,000 rpm, 10 min). The supernatant was diluted and used for analysis.

Qualitative UPLC-Q/TOF-MS analysis was performed using an Agilent Zorbax Extend C_{18} UHPLC column (2.1 × 100 mm, 1.8 μm). The MS scanning mode and TOF-MS conditions used were as previously described.[19] Separation was performed via linear gradient elution, using a mobile phase consisting of 0.1% (v/v) aqueous formic acid (A) and acetonitrile (B), with the optimized program conditions set as follows: 0.1–3 min, 95–85% A; 3–7 min, 85–80% A; 7–8 min, 80–65% A; 8–10 min, 65% A; 10–11 min, 65–25% A; 11–18 min, 25–5% A; 18–20 min, 5% A; 20–22 min, 5–95% A; and 22–24 min, 95% A.

Data processing included database establishment, compound identification, data pre-processing, chemical pattern recognition analysis, and screening of differential metabolites. Compounds were identified using Peak View 1.2 software. Marker View 1.2 and SIMCA 14.1 software were used for screening metabolites for variable importance in projection (VIP) >1. Further analyses were performed using https://www.metaboanalyst.ca/MetaboAnalyst/home.xhtml. The target compounds were defined as $|\log_2(\text{fold change})| > 1$.

Co-Incubation of Gut Microbiota in vitro

Fecal samples from the OVX rats were homogenized and centrifuged (5000 rpm, 5 min) to obtain the supernatants, which were subsequently added to Gifu Anaerobic Medium (GAM) and incubated at 37°C for 24 h in an anaerobic incubator (AW200SG, Electrotec, Colchester, UK). The QEP extracts were prepared according to the method described in "Preparation and Analysis of QEP". The QEP extract concentrations were adjusted for oral gavage treatment. The incubation systems were configured with concentration gradients of 1.8 mg/mg (QEP/feces). The initial bacterial solution was inoculated into blank GAM and conditioned media with QEP. After 48 h of incubation, the culture was centrifuged (6000 rpm, 5 min), and the resulting bacterial pellets were collected for 16S rRNA sequencing.

Statistical Analysis

GraphPad Prism 8.0.2 was used for all statistical analyses. All experimental data are expressed as the mean ± standard deviation. Unless otherwise stated, statistical tests were performed using one-way analysis of variance (ANOVA). Correlation analysis was performed using the OmicStudio platform (https://www.omicstudio.cn/home).

Results

QEP Improved Bone Mineral Density and Bone Biomechanical Properties in OVX Rats

To investigate whether QEP exerts osteoprotective effects, we conducted daily gavage administration of QEP to OVX rats for 6 weeks (Figure 1A). Initially, estrogen deficiency led to significant weight gain, which was significantly faster increases in OVX rats, and QEP treatment does not significantly ameliorate weight gain. (Figure 1B). Under estrogen-deficient conditions, the uterine index (uterine weight/body weight) of rats was significantly decreased, suggesting that uterine growth was inhibited. By contrast, the uterine index of QEPH-treated rats was significantly increased, whereas

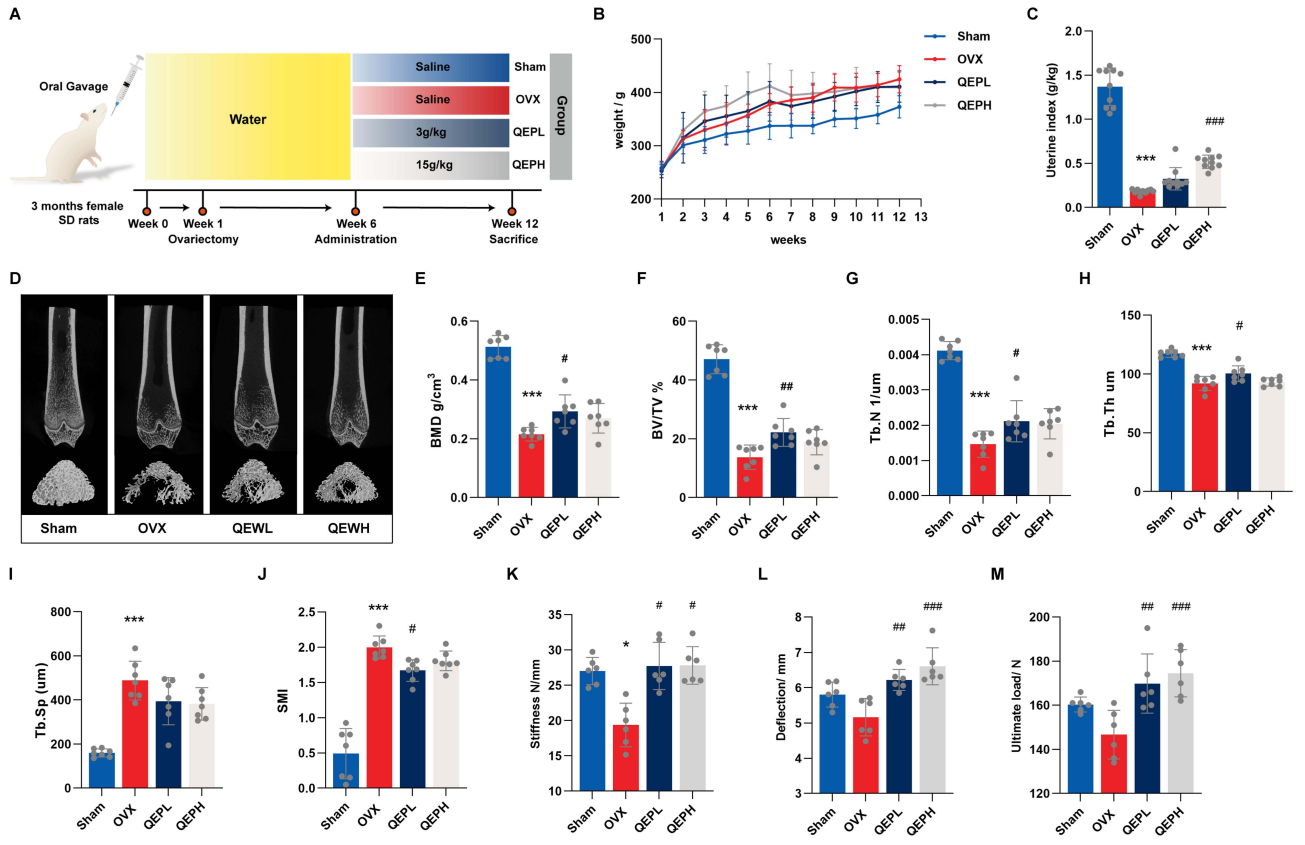

Figure 1 QEP improved bone microstructural and biomechanical properties. (**A**) Schematic diagram of the animal experiment design. (**B**) Body weight trend. (**C**) Uterine index (uterine weight/body weight) (n = 10). (**D**) 3D longitudinal and transverse sections of the distal femur of rats were determined by MicroCT. (**E–J**) BMD, BV/TV, Tb.N, Tb.Th, Tb.Sp, and SMI measurements (n = 7). (**K–M**) Femur stiffness, deflection, and ultimate load (n = 6). *$P < 0.05$, ***$P < 0.001$, vs Sham; $^{\#}P < 0.05$, $^{\#\#}P < 0.01$, $^{\#\#\#\#}P < 0.001$, vs OVX.

there was no significant change in the uterine index of QEPL-treated rats, which may be related to the amount of estrogen-like effector components in QEP. (Figure 1C).

Next, in order to investigate the effect of QEP on the bone microstructure of the femur in OVX rats, we visualized it by Micro-CT, for obtaining the trabecular microstructure of the distal femur in three dimensions. Obviously, OVX led to decreased trabecular density, a disorganized trabecular arrangement, and an expanded marrow cavity; treatment with QEP significantly improved the trabecular microarchitecture (Figure 1D). Additionally, QEPL was able to significantly improve the BMD, BV/TV, Tb.N, Tb.Th, and SMI, and QEPH had a weaker anti-osteoporosis effects compared to QEPL (Figure 1E–J). Notably, impaired trabecular structure can affect the load-bearing capacity and brittleness of the bone. The three-point bending test can be used to assess the biomechanical properties of bone, reflecting the strength and toughness of bone, and is an important indicator for evaluating osteoporosis. As shown in Figure 1K–M, QEP could mitigate the detrimental effects of estrogen deficiency on bone strength; enhancing bone stiffness, deflection, and ultimate load. Thus, these results suggested that QEP improved bone mineral density and bone biomechanical properties in OVX rats and low dose QEP exhibited preferable therapeutic effects.

QEP Improves Histopathological Damage, and Modulates Serum Bone Biochemical Indicators in OVX Rats

Tartrate resistant acid phosphatase (TRAP) is a marker enzyme for osteoclasts and is specifically distributed in osteoclasts. TRAP staining of femoral tissues showed that the OVX group had more osteoclasts and more disorganized and sparsely distributed bone tissue compared to the Sham group, and QEP had effectively attenuated estrogen deficiency-induced osteoclastogenesis (Figure 2A and B). In terms of bone biochemical indicators, ovariectomy

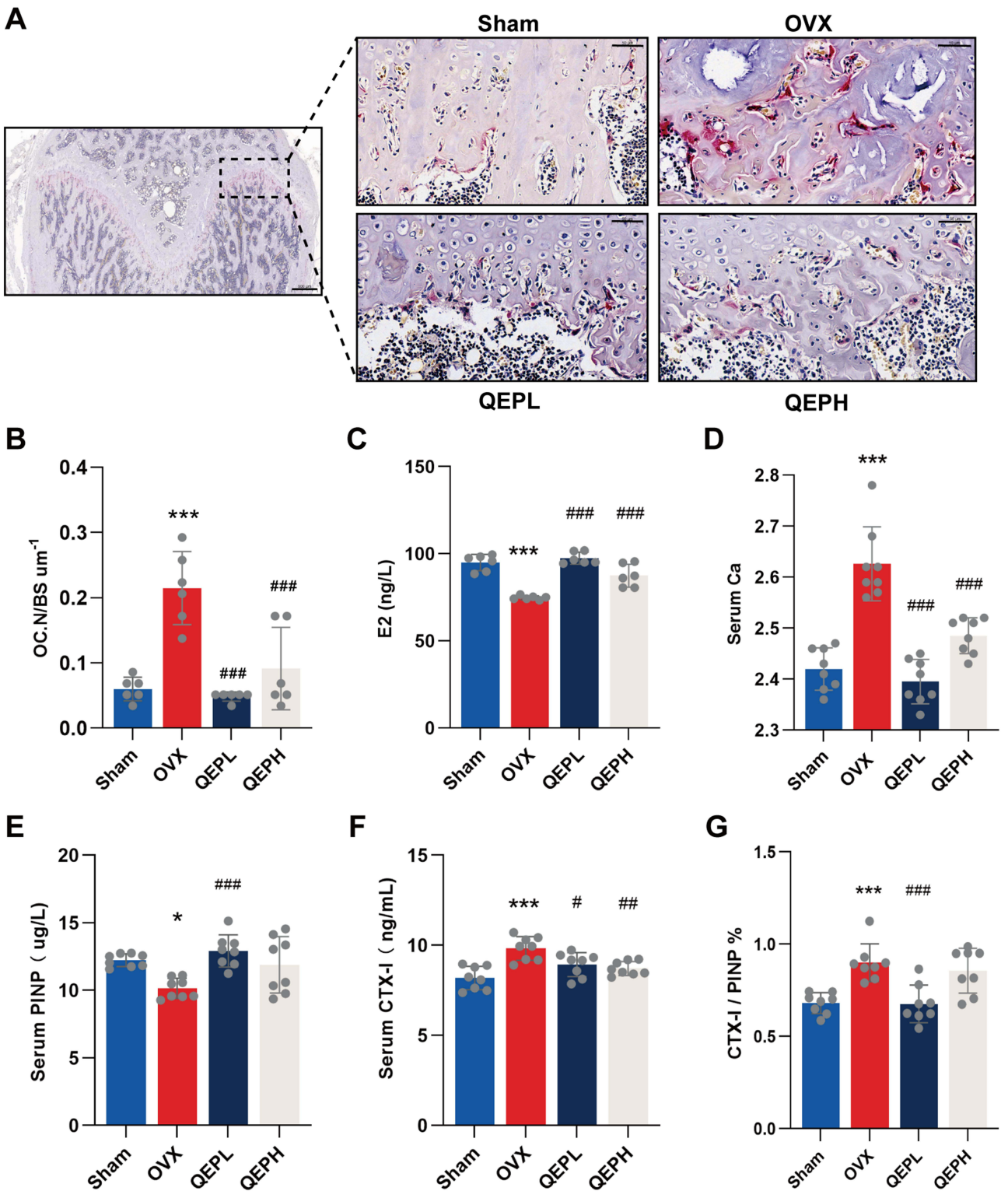

Figure 2 QEP improves histopathological damage and serum bone biochemical indicators. (**A**) Representative TRAP-stained images (red scale bar, 500 μm; enlarged figure, 50 μm). (**B**) Number of osteoclasts per millimeter of bone surface (OC.N/BS) for TRAP staining in the femur (n = 3). (**C**–**F**) Serum E2, Ca, PINP, and CTX-I levels (n = 6–8). (**G**) CTX-I/PINP (%) (n = 7). *P < 0.05, ***P < 0.001, vs Sham; $^{\#}P$ < 0.05, $^{\#\#}P$ < 0.01, $^{\#\#\#}P$ < 0.001, vs OVX.

significantly reduced the serum Estradiol (E2) levels, which were significantly increased in QEP rats (Figure 2C). The serum calcium levels were also significantly reduced in the QEP groups (Figure 2D), suggesting that QEP was effective in reducing bone resorption levels. Furthermore, relative to the Sham group, the OVX group displayed notable reductions

https://doi.org/10.2147/JIR.S517176

in procollagen type I N-terminal propeptide (PINP) levels, alongside a significant increase in C-telopeptide of type I collagen (CTX-I) levels, indicating ovariectomy increases bone turnover levels in rats. QEPL elevated the levels of (PINP) and reduced those of (CTX-I); therefore, the imbalanced CTX-I/PINP, bone turnover rate had been significantly *regressed* (Figure 2E–G). Additionally, QEPH-treated rats showed a notable decrease in CTX-I levels.

QEP Restored Intestinal Barrier in OVX Rats

In the oestrogen-deficient state, the gut immune status is a very important cause of bone loss due to the migration of immune cells or inflammatory cytokines. The intestinal barrier plays a crucial role in maintaining intestinal and systemic immune responses. Damage to the intestinal barrier can lead to increased intestinal permeability, which in turn upregulates the intestinal inflammatory response, ultimately affecting bone density[20] plays a crucial role in upregulating inflammation. As shown in Figure 3A, clear and distinct layers of the colonic mucosa, muscular mucosa, submucosa, and muscular layer with abundant well-arranged crypts were observed in the Sham group. By contrast, the OVX group of rats exhibited evident local mucosal damage, the atrophy and deformation of the intestinal glands, the destruction of crypts, and the infiltration of inflammatory cells. QEP mitigated the mucosal injury, improved the crypt structure, and reduced inflammatory cell infiltration (Figure 3B). Furthermore, the serum LPS levels were significantly reduced in the QEP groups, suggesting that QEP treatment can alleviate the inflammatory response caused by intestinal barrier injury to a certain extent. (Figure 3C).

QEP Restored the Balance of Th17/Treg and the Levels of Related Cytokine in MLN

To further explore changes in the inflammatory response due to intestinal barrier injury before and after QEP intervention, we observed changes in the balance of Th17/Treg and the levels of related cytokine in MLNs. Compared with the Sham group, the mRNA expression levels of *RORγt* and *IL-17A* in the colon of OVX rats were significantly increased, whereas the QEP reduced the transcription of Th17-related genes (Figure 4A and B). Moreover, *Foxp3* mRNA expression was also reduced in the colon of OVX rats, and QEP treatment increased it (Figure 4C). Furthermore, the percentage of $CD4^{+}IL\text{-}17A^{+}$ Th17 cells was increased in the MLNs of OVX rats, whereas the percentage of $CD4^{+}CD25^{+}$ Foxp3+ Treg cells was significantly decreased. Notably, QEP

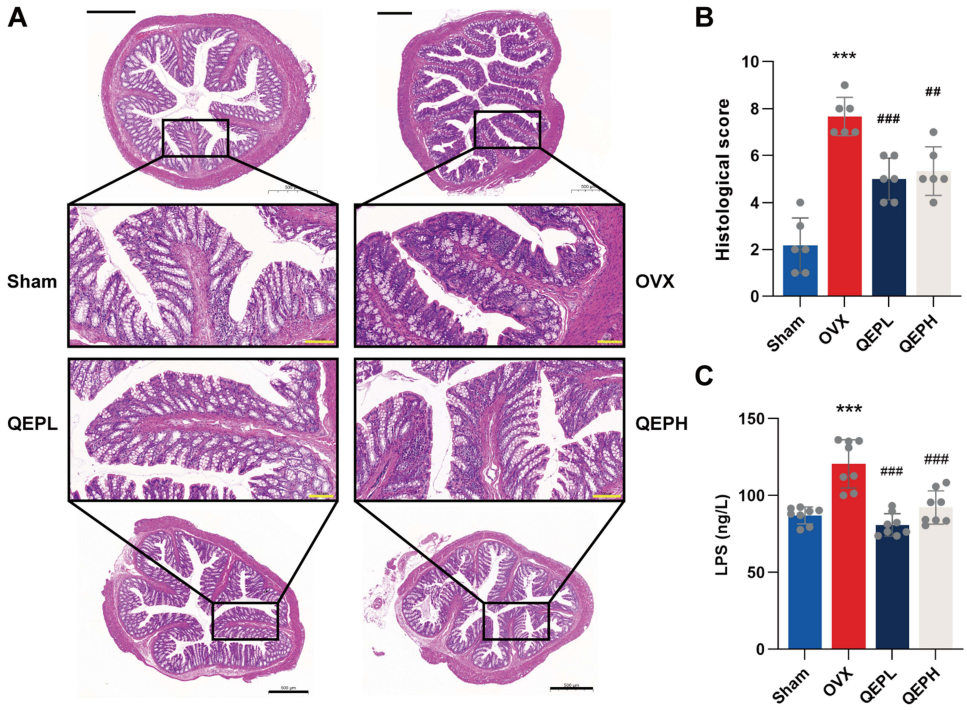

Figure 3 QEP restored intestinal barrier. (**A**) Representative images of H&E-stained in colon tissue (black scale bar, 500 μm; enlarged figure, 100 μm). (**B**) Histological disease scores (n = 3). (**C**) Serum LPS levels (n = 8). ***$P < 0.001$, vs Sham; $^{\#\#}P < 0.01$, $^{\#\#\#}P < 0.001$, vs OVX.

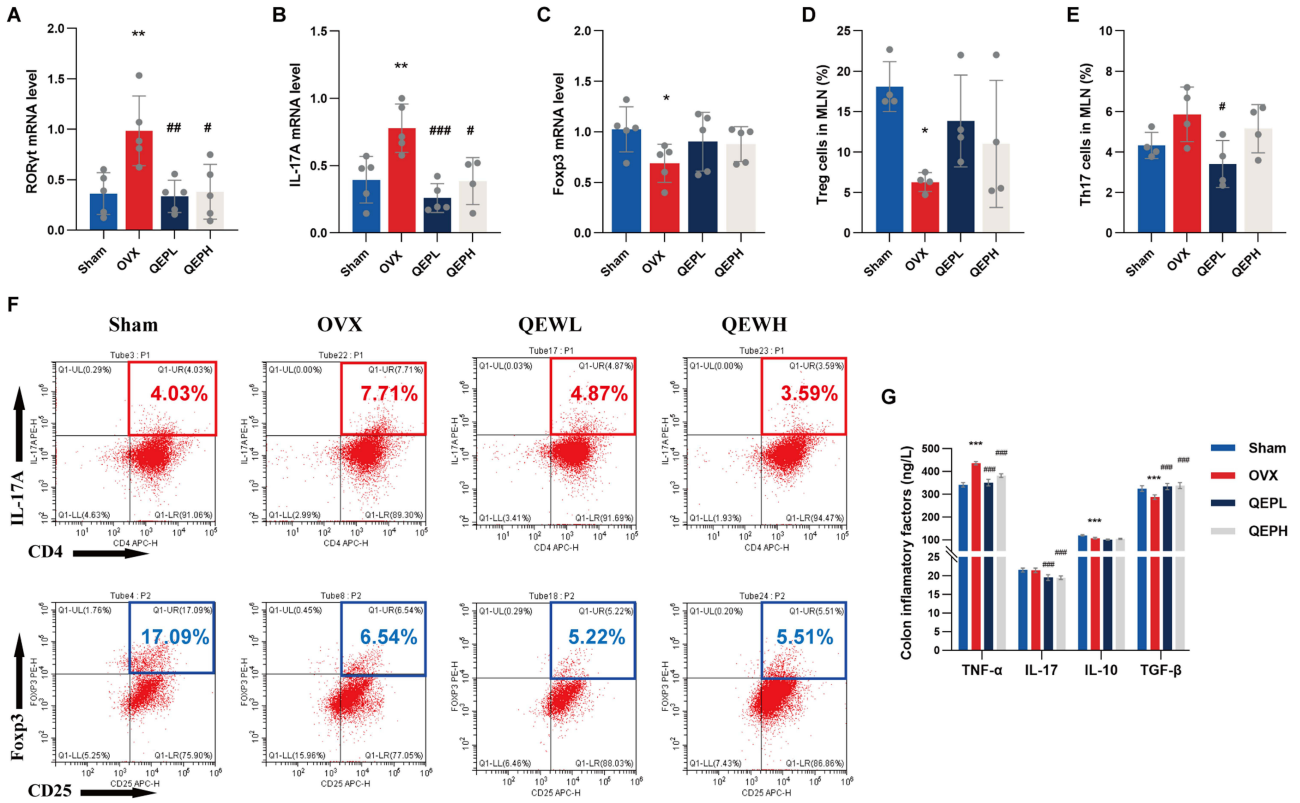

Figure 4 QEP restored the balance of Th17/Treg and the levels of related cytokine in MLN. (**A**–**C**) Quantification of the *RORγt, IL-17A*, and *Foxp3* mRNA levels in the colon (n = 5). (**D** and **E**) Proportion of Treg and Th17 cells in MLN (n = 3). (**F**) Representative flow cytometric cell sorting diagram of Treg and Th17. (**G**) Expression levels of colonic inflammatory cytokines (n = 6, Dunnett multiple comparisons test). $^{*}P < 0.05$, $^{**}P < 0.01$, $^{***}P < 0.001$, vs Sham; $^{\#}P < 0.05$, $^{\#\#}P < 0.01$, $^{\#\#\#}P < 0.001$, vs OVX.

treatment restored the Th17/Treg balance to some extent (Figure 4D–F). We further detected the colonic expression of inflammatory cytokines, that of colonic TNF-α was significantly increased in the OVX rats, but this upregulation effect was significantly attenuated by QEP treatments. Consistently, QEP treatment significantly attenuated the expression of IL-7. Furthermore, the levels of IL-10 and TGF-β were significantly decreased in OVX rats, but the QEP significantly increased that of TGF-β (Figure 4G).

QEP Restored the Balance of Th17/Treg and the Levels of Related Cytokine in Bone

To further explored whether estrogen deficiency leads to similar Th17/Treg expression in bone as in the gut, we measured the expression of Th17/Treg in the femur of the groups. QEP intervention significantly regulated the balance of Th17/Treg (Figure 5A and B). Meanwhile, the expression of Th17/Treg-related inflammatory cytokines in the bone marrow was also examined (Figure 5C). The expression of IL-17 and TNF-α was significantly increased in the OVX group, which was attenuated by QEP treatment. Furthermore, the expression of the anti-inflammatory cytokines TGF-β and IL-10 was significantly decreased in the OVX group, a pattern that was reversed by QEP treatment, suggesting that QEP also had an ameliorative effect on the state of inflammation in bone. Additionally, the QEP significantly downregulated Receptor Activator for Nuclear Factor-κ B Ligand (RANKL) expression in the OVX rats. This observation was consistent with the corresponding trend in colonic Th17/Treg alteration.

QEP Enhanced Species Diversity of Gut Microbiota in OVX Rats

To assess the effects of QEP on gut microbiota compositions in OVX rats, the V3-V4 regions of the 16S rRNA gene were sequenced. The dilution curve exhibited a flattening trend, indicating that the sample size was sufficiently large and representative of microbial diversity (Figure 6A). Moreover, both the richness and diversity of gut microbiota in OVX rats were reduced, and QEPH specifically causing a significant decrease in alpha diversity (Figure 6B), which may

https://doi.org/10.2147/JIR.S517176

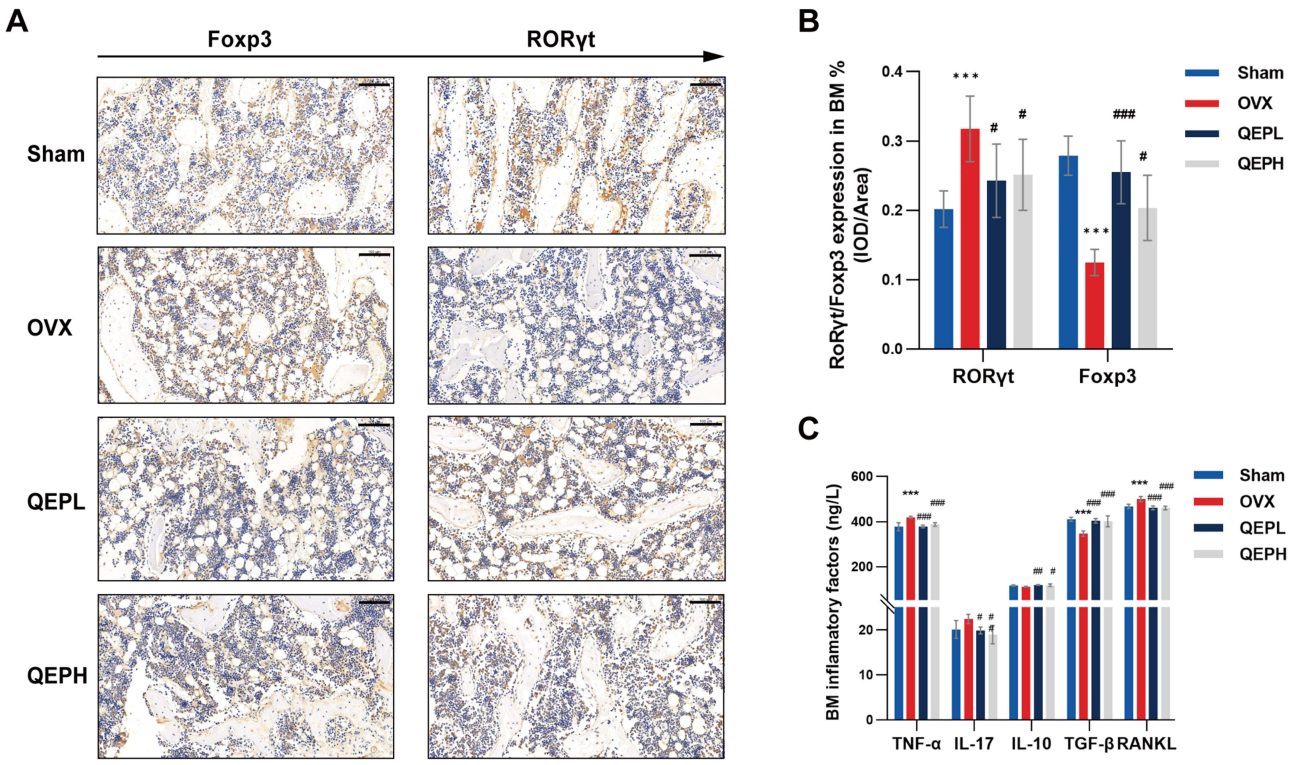

Figure 5 QEP restored the balance of Th17/Treg and the levels of related cytokine in bone. (**A** and **B**) Representative images of immunohistochemical staining and integrated optical density (IOD) /area of RORγt and FOXP3 in the femur (scale bar, 100 μm; Dunnett multiple comparisons test). (**C**) Expression levels of inflammatory cytokines in the bone marrow (n = 6, Dunnett multiple comparisons test). $^{***}P < 0.001$, vs Sham; $^{\#}P < 0.05$, $^{\#\#}P < 0.01$, $^{\#\#\#\#}P < 0.001$, vs OVX.

explain why increasing the dose of QEP did not enhance its efficacy. Combined the effects of anti-osteoporosis, QEPL was expected to have better effects on the gut microbiota. Then, the partial least squares-discriminant analysis (PLS-DA) (Figure 6C) and principal coordinate analysis (PCoA) (Figure 6D) results demonstrated a significant divergence in microbial composition between the Sham and OVX groups on an operational taxonomic unit (OTU) level. Consistent with its effect on the alpha diversity, QEPH caused further differentiation from other taxa. Analysis of similarity (ANOSIM) further revealed significant differences between the groups (Figure 6E). Additionally, the results of PLS-DA and ANOSIM at the genus level are shown in Figure 6F and G, with similarity of the OTU level. Based on the relative abundance of microorganisms at the genus level, the Sham and QEPL groups were clustered based on their dominant genus, *Lactobacillus* (Figure 6H). The findings suggested that estrogen deficiency resulted in a decrease in the diversity of the gut microbiota. In contrast, QEP treatment effectively enhanced species diversity, aligning it more closely with the levels observed in the Sham group.

QEP Alter the Species Composition of Gut Microbiota in OVX Rats, Particularly of *Lactobacillus*

We assessed the relative abundance of dominant species at the phylum, family, and genus levels, for determining the effects of QEP on gut bacterial abundance. As shown in Figure 7A, the dominant phyla were Firmicutes and Bacteroidetes. At the family level (Figure 7B), OVX rats showed decreased relative abundances of Lactobacillaceae, Ruminococcaceae, Peptostreptococcaceae, Erysipelotrichaceae, and norank_o_Clostridia_UCG-014 compared with the Sham group levels, whereas these bacterial changes were partially reversed by QEPL treatment. Notably, unlike the QEPL-affected trends, QEPH significantly increased the relative abundances of Bacteroidaceae and Muribaculaceae and decreased that of norank_o_Clostridia_UCG-014. However, the effects of QEPL and QEPH on the other major dominant species showed the same trend but to different extents. At the genus level (Figure 7C), estrogen deficiency resulted in a significant decrease in the relative abundances of *Lactobacillus, norank_f_norank_o_Clostridia_UCG-014,*

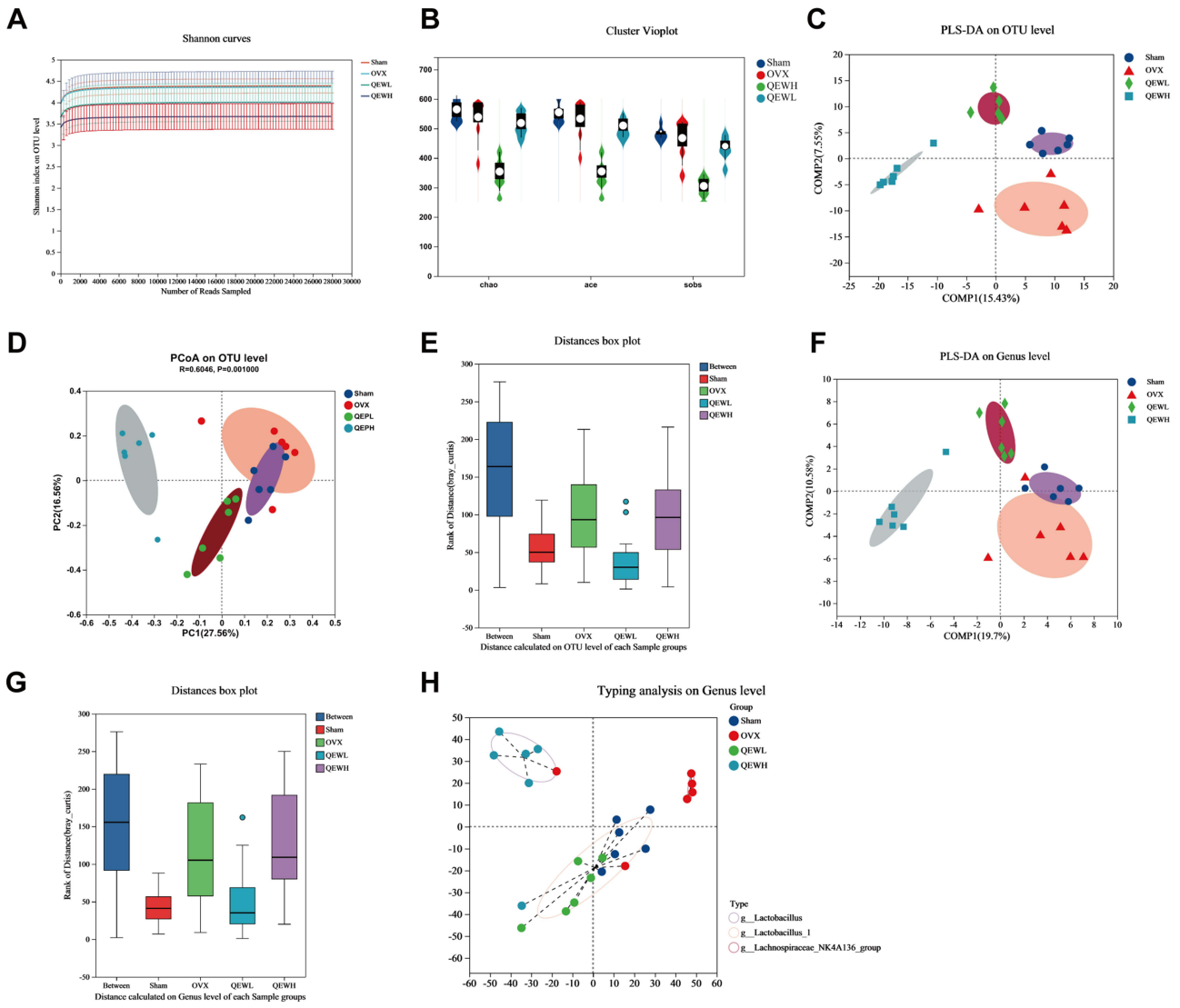

Figure 6 QEP enhanced species diversity of gut microbiota. (**A**) Dilution curve. (**B**) Alpha diversity. (**C**–**E**) Beta diversity analysis by PLS-DA, PCoA, and ANOSIM on OTU level. (**F** and **G**) PLS-DA, ANOSIM analysis at the genus level. (**H**) Gut microbiota typing analysis at the genus level.

Romboutsia, and *Turicibacter*, and increased those of *unclassified_f_Lachnospiraceae, Bacteroides, UCG-005*, and *Lachnospiraceae_NK4A136_group*. However, QEPL treatment restored the imbalance of the intestinal flora shown in the OVX group. By contrast, QEPH increased the relative abundances of *norank_f_Muribaculaceae* and *Bacteroides* and significantly decreased that of *norank_f_norank_o_Clostridia_UCG-014*. The variations in each sample are illustrated in Figure S2A–C. Notably, *Lactobacillus* tended to emerge as a dominant species.

Furthermore, multiple-group comparisons revealed trends in the relative abundances of the top 30 genera, *Lactobacillus* is the species with the highest abundance ratio, indicating that it plays a potential role in maintaining intestinal homeostasis as an intestinal probiotic (Figure 7D). Consistently, the comparisons between OVX and QEPL also revealed that the *Lactobacillus* was the most prominent species in terms of species abundance and differential characteristics (Figure 7E and F).

QEP Modulated Gut Microbiota of OVX Rats in vitro, Particularly of *Lactobacillus*

To delve deeper into the mechanisms by which QEP modulates the gut microbiota and to search for potential target probiotics that are directly affected by QEP. We conducted an in vitro co-cultivation of fecal samples from OVX subjects

https://doi.org/10.2147/JIR.S517176

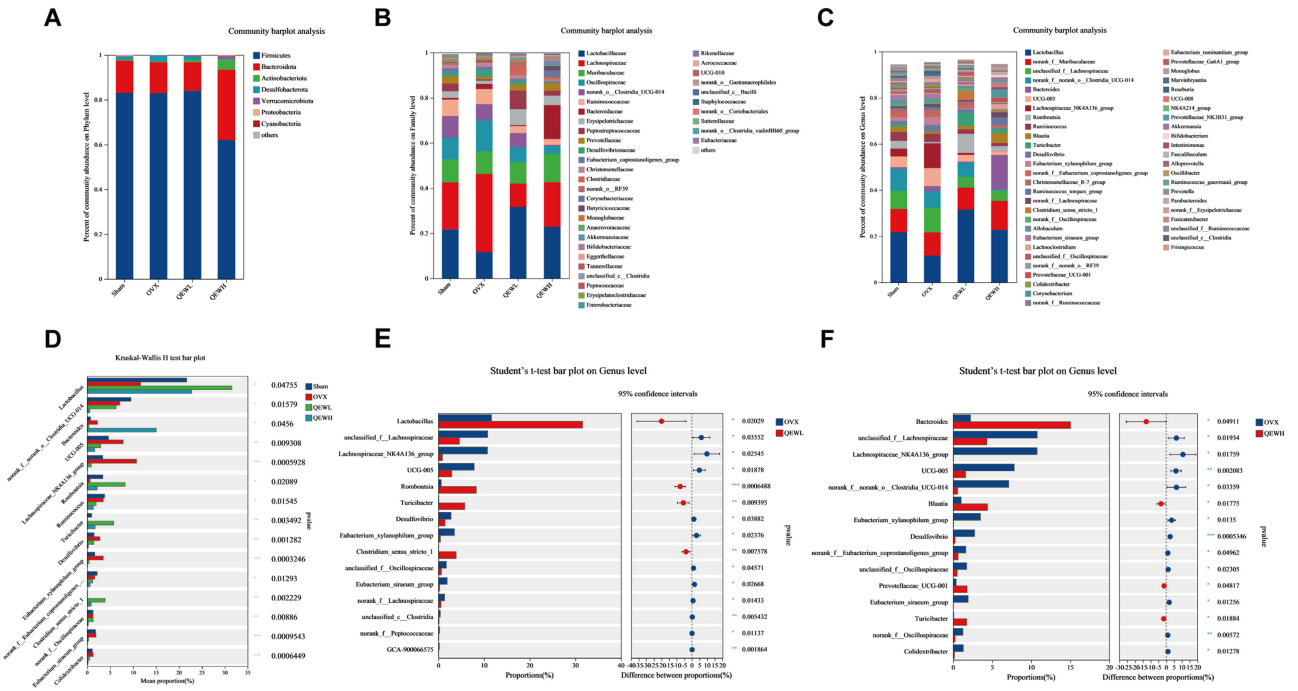

Figure 7 QEP alter the species composition of gut microbiota. (**A**–**C**) Relative abundances of gut microbes at the phylum, family, and genus levels. (**D**) Comparative analysis of species abundances in all groups. (**E**) Comparative analysis of species abundances between the OVX and QEPL groups (**F**) OVX and QEPH (n = 6).

with conditioned medium that contained either QEP or not. Subsequently, the alterations in the gut microbiota as a result of the effect of QEP were meticulously assessed using 16S rRNA gene sequencing analysis.

According to the Simpson index (Figure 8A), the administration of QEP significantly increased the alpha diversity of the gut microbiota of OVX rats in vitro. Principal co-ordinates analysis (PCoA) (Figure 8B) demonstrated that the taxa of the QEP group was clearly distinguishable from OVX group, with stable uniformity. Analysis of similarities (ANOSIM) (Figure 8C) similarly revealed significant group differences. The microbial dysbiosis index (Figure 8D) showed that QEP had a superior effect on alleviating gut microbiota disruption. At the genus level (Figure 8E and F), both the QEP group and the OVX group exhibited a lower number of species, probably due to the culture condition and competition between intestinal flora, but the species structural compositions of the individual samples in the QEP group were more uniformly and stably distributed. Furthermore, *Lactobacillus* was the most dominant genus, occurring at a significantly higher level than that in the OVX group, which agreed with the in vivo results. Additionally, comparisons between OVX and QEP groups showed that the most prominent differentiating genus in vitro was *Lactobacillus* (Figure 8G). Thus, QEP exerted significant beneficial effects on the gut microbiota of OVX rats in vitro and significantly increased the abundance of *Lactobacillus*. *Lactobacillus* may be the potential target genus in the alleviation of osteoporosis in OVX rats by QEP.

QEP Regulated Fecal Metabolomics of OVX Rats

Next, the alterations of the gut microbiome encouraged us to explore the related metabolites influenced by OVX and QEP. According to the results of analysis of the microbial communities, a low dose of QEP modulated the species composition of the intestinal flora more significantly toward the Sham group and significantly increased alpha diversity. At the genus level, the abundance of *Lactobacillus* was significantly increased. Therefore, in the subsequent untargeted metabolomics study on fecal samples, we focused on comparing the Sham, OVX, and QEPL groups. The representative UHPLC-Q-TOF MS chromatograms for the Sham, OVX and QEPL groups in positive and negative ion modes were illustrated in Figure 9A and B. Principal component analysis (PCA) was applied to visualize the overall metabolic discrepancies among the groups. Obviously, the OVX and Sham group separated, while the QEPL intervention altered the metabolic characteristics of OVX significantly too similar to Sham (Figure 9C and D). Similarly, the analysis of orthogonal partial least squares discriminant analysis (OPLS-DA) also indicated the distinct separation, with significant

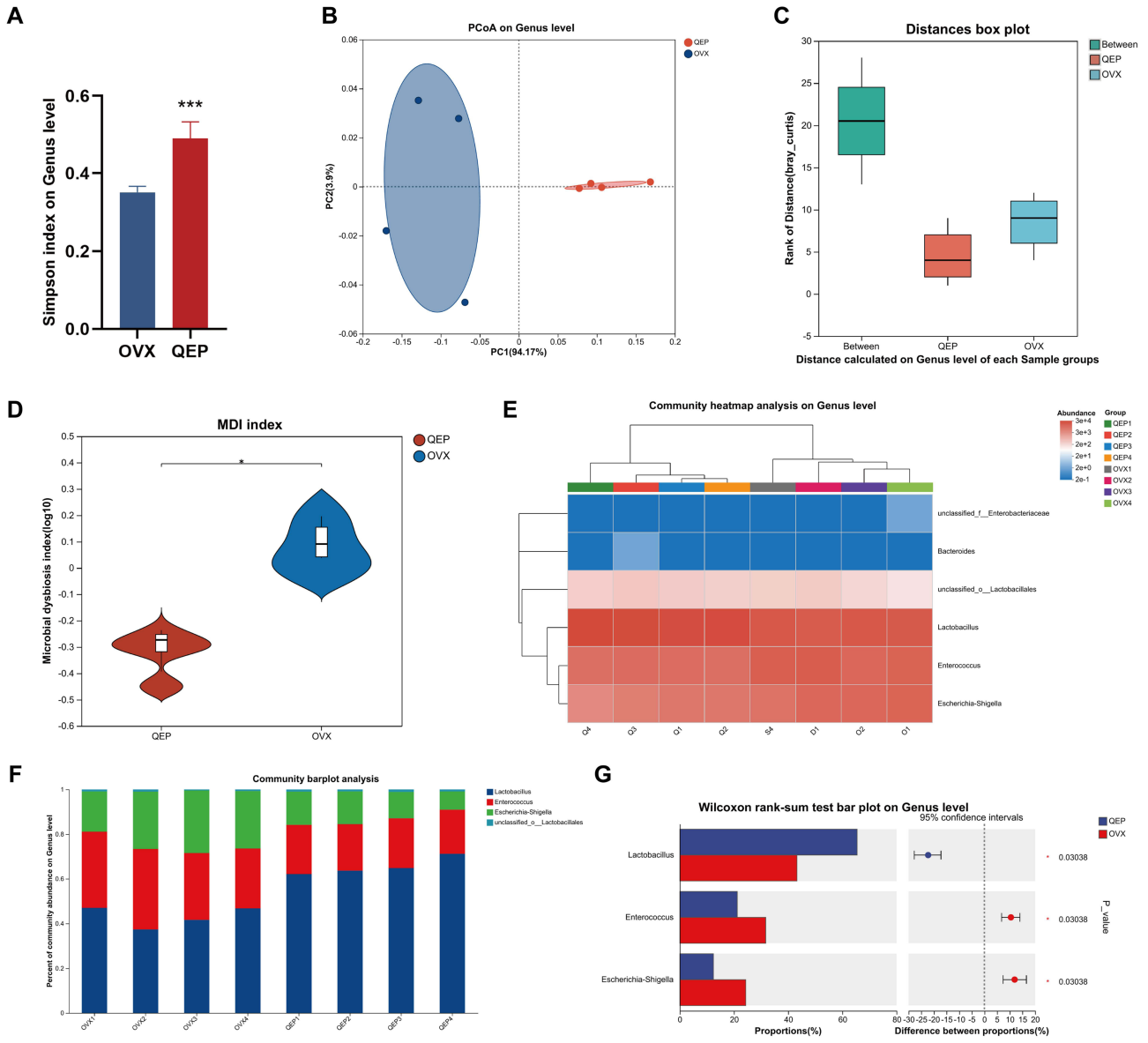

Figure 8 QEP plays an important role in regulating the gut microbiota in vitro. (**A**) Simpson index (n = 4). (**B** and **C**) Beta diversity analysis by PCoA and ANOSIM at the genus level. (**D**) Microbial dysbiosis indexes. (**E**) Heat map at the genus level. (**F**) Community abundances at the genus level. (**G**) Wilcoxon rank-sum test bar plot on genus level (n = 4). ***$P < 0.001$, vs OVX.

metabolic differences between OVX and QEPL groups (Figure 9E and F). Additionally, a crucial step was the screening of significantly differential metabolites. The volcano plot analysis revealed a set of 107 metabolites in positive ion mode and 158 in negative ion mode that showed significant differences between the OVX and QEPL groups. Among these, 205 metabolites were significantly upregulated, whereas 60 were downregulated, as depicted in Figure 9G and H. Furthermore, metabolites that exhibited alterations following QEPL treatment were identified based on the stringent criteria: P-values of <0.05, VIP values of >1 and $|\log_2(FC)|$ values of >1. Through the selection process, we ultimately identified 71 fecal metabolites with significant variations across the groups (Table S2). Further enrichment analysis of the differential metabolites between the OVX and QEPL groups via MatabolAnlyse 5.0 uncovered several pivotal metabolic pathways, including estrone metabolism, steroidogenesis, androgen and estrogen metabolism, androstenedione metabolism and alpha linolenic acid and linoleic acid metabolism (Figure 9I).

https://doi.org/10.2147/JIR.S517176

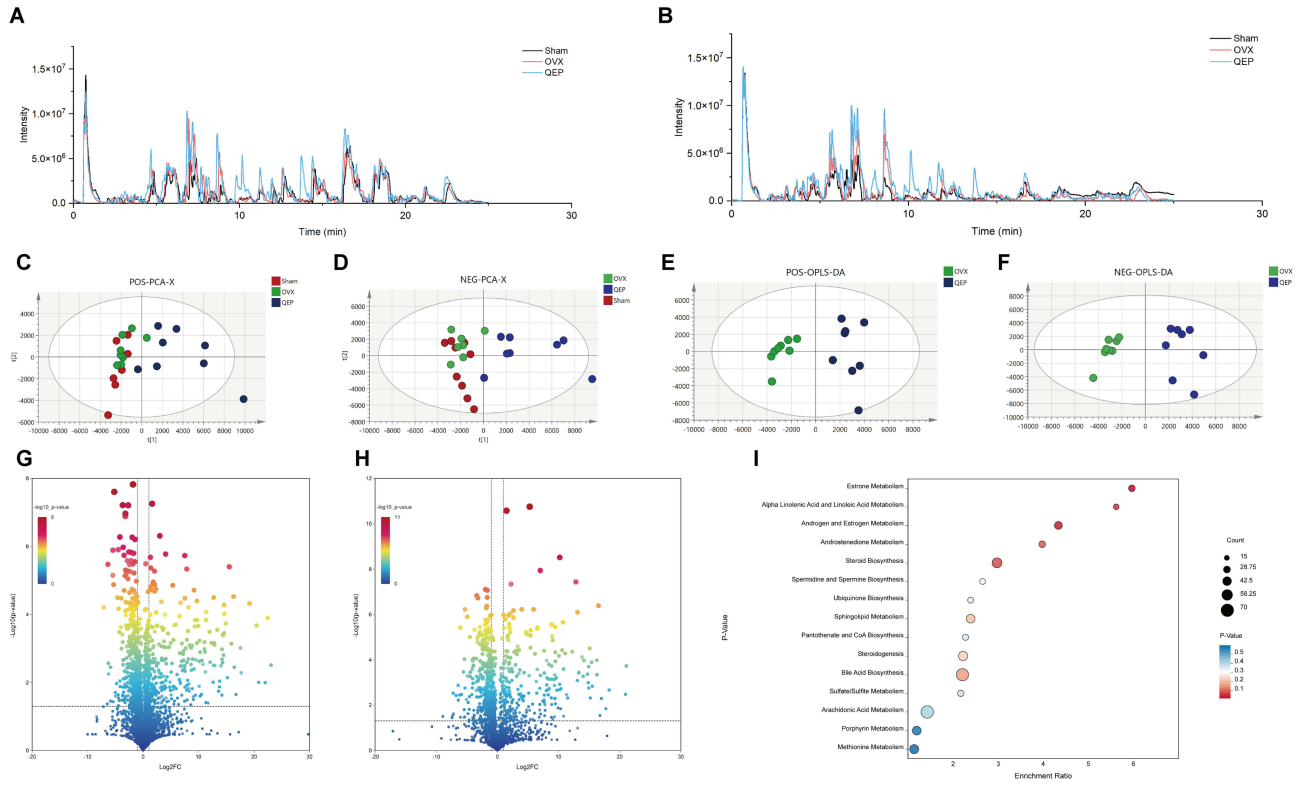

Figure 9 Fecal metabolic profile was altered by QEP administration. (**A** and **B**) Total ion chromatograms in positive and negative ion mode. (**C** and **D**) Scores plot of PCA analysis in positive and negative ion mode. (**E** and **F**) OPLS-DA analysis in positive and negative ion mode. (**G** and **H**) Volcano map analysis of OVX Vs QEP groups in positive and negative ion mode. (**I**) The KEGG pathway enrichment analysis of the differential metabolites in the OVX Vs QEP groups.

Correlation Analysis Among Metabolites, Gut Microbiota, and Th17/Treg-Related Indexes

Notably, QEP regulated the correlation between estrogen deficiency-induced Th17/Treg imbalance and the gut microbiota. The bone biomechanical indicators, PINP, TGF-β, and IL-10 were clustered together, which were clustered into one group with Tb.Th, Tb.N, BMD, and BV/TV. The main bone trabecular microstructural indicators, SMI, Tb.Sp, CTX-I, and CTX/PINP, Ca as well as IL- 17 and TNF-α were clustered together, which were mainly associated bone resorption (Figure 10A). Bone resorption factors were negatively correlated with the abundances of Erysipelotrichaceae, Clostridiaceae, Eggerthellaceae, Lactobacillaceae, and Peptostreptococcaceae. Additionally, Lachnospiraceae, Desulfovibrionaceae, Peptococcaceae, Oscillospiraceae, and unclassified_c_Clostridia correlated positively with bone resorption and negatively with osteogenesis (Figure 10B). The correlation trends at the genus level were similar to those at the family level (Figure 10C). These results illustrate the potential role of *Lactobacillus* in the improvement of osteoporosis by QEP.

To further clarify the potential functional relationship disturbed differential metabolites, altered gut microbes and changed pathological indicators related to bone metabolism and immunity, we analyzed the correlation among the three using the Pearson correlation algorithm. We analyzed the correlation between the screened differential metabolites and the differential flora of the top 12 QEPL and OVX, as well as BMD, PINP, CTX-I, BM IL-10, BM TGF-β, BM TNF-α, BM IL-17 and BM RANKL. Figure 10D was generated to reflect the different relationships. The core genera with a high impact ($p < 0.01$) were *Lactobacillus*. Collectively, we revealed the potential role of gut microbiota interacting with Th17/Treg balance and other biomarkers on the anti-osteoporotic effects of QEP.

Figure 10 The potential relationship between metabolites, gut microbiota and Th17/Treg-related indexes. (**A**) Heat maps of bone indexes and Th17/Treg ratios. (**B** and **C**) Correlation of gut microbes with bone indexes and Th17/Treg ratios at the family and genus level. *P < 0.05, **P < 0.01, ***P < 0.001, purple indicates a positive correlation and green indicates a negative correlation. (**D**) Mantel test correlation diagram. *P < 0.05, **P < 0.01, ***P < 0.001, red indicates a positive correlation and blue indicates a negative correlation.

Discussion

The global prevalence of osteoporosis is increasing with rising life expectancy and a growing elderly population. Osteoporosis is the most common metabolic bone disease and characterized by impairment of bone structure, reduced bone mechanical properties and increased bone fragility, leading to increased risk of fragility fractures.[21] The use of currently clinically preferred anti-osteoporotic drugs such as bisphosphonates (alendronate, risedronate) is often associated with severe musculoskeletal pain, osteonecrosis of the jaw, femoral fractures, and upper gastrointestinal adverse effects.[22] QEP is now mostly used clinically for the treatment of postmenopausal osteoporosis with favorable efficacy. Our study investigated the mechanism of action of QEP in the treatment of postmenopausal osteoporosis. Here, we found that QEP had significant improvement effects on bone mineral density and bone microstructure as well as bone biomechanical strength in OVX rats. In addition, QEP significantly improved the intestinal barrier, intestinal microbial disorders and the balance of Th17/Treg in the gut-bone axis.

In recent years, many studies have confirmed the crucial role of gut microbes in the development of postmenopausal osteoporosis play. In sex steroid depleted mice, disturbed gut microbes may lead to increased intestinal permeability and trigger activation of important inflammatory pathways, further contributing to bone loss, while germ free mice are

https://doi.org/10.2147/JIR.S517176

protected from such effects.[8,23,24] At the phylum level, the Firmicutes and Bacteroidetes phyla were dominant in the Sham and OVX groups.[25–27] Compared with Sham mice, OVX-induced osteoporosis mice showed significant increases in the gut bacteria belonging to the Muribaculaceae, Bifidobacteriaceae, and Clostridiaceae families. Especially, the relative abundances of the family Lactobacillaceae and genus *Lactobacillus* were markedly downregulated in the cecal contents of OVX mice in comparison with Sham mice.[28] Consistent with our previous study, we found that the dominant phyla were Firmicutes and Bacteroidetes in all group. Among the top 30 differential genera, *Lactobacillus* exhibited the highest abundance ratio, and QEP directly increased the abundance of *Lactobacillus* in vivo, suggesting that *Lactobacillus* may play a significant role in osteoporosis.[18] In addition, 16S rRNA analysis of co-culture of QEP with OVX rat feces revealed that QEP could also directly increase the abundance of *Lactobacillus* in vitro. The stability and reproducibility of the changes induced by QEP in *Lactobacillus* were higher than those observed in all other genera, thereby further confirming that *Lactobacillus* is a potential target genus for the action of QEP. The regulatory effects of QEP on gut microbiota composition may stem from its fatty acid constituents, flavonoid, and polysaccharide. The *J. regia* in QEP contains abundant polyunsaturated fatty acids with a uniquely high ω3: ω6 ratio, which can regulate the gut microbiota, and affect the proinflammatory mediators, such as IL-17.[29,30] Furthermore, it has shown that supplementation with unsaturated fatty acids directly increases the abundance of *Lactobacillus*.[31,32] Notably, a substantial proportion of flavonoids in QEP are predominantly derived from *P. corylifolia*. As prebiotics, these flavonoids play an important role in gut microbes by regulating the composition and the diversity of gut microbiota, protecting intestinal barrier function, regulating the immune system, and affecting the metabolites of gut microbiota.[33] In addition, the functional homogeneous polysaccharide from the *E. ulmoides*, was shown to exhibit anti-OP effects through its influence on gut microbiota composition and serum metabolites.[34]

Furthermore, we found a significant increase in *Bacteroides* in the QEPH-treated rats. *Bacteroides* are primary candidates for next-generation probiotics. The beneficial effects of *Bacteroides vulgatus* on colonic microbiota dysregulation and lumbar bone loss in OVX mice has already been established.[35] Additionally, extensive evidence has demonstrated the effects of *Bacteroides* in alleviating inflammation and intestinal injury.[36] We observed a more favorable pharmacodynamic profile for QEPL (more closely related to the dose actually administered in the clinic) compared to QEPH, and differences in QEPL and QEPH effects on the gut microbiota in vivo were obvious. Therefore, the mechanisms of action of QEP at different doses may differ. Considering that the drug viscosity of a high dose may have a certain effect on the gastrointestinal tract, more dose-based studies should be carried out.

In addition to the gut dysbiosis, recent studies on osteoporosis have increasingly focused on bone immunity because of the close interactions and crosstalk between bone and immune cells.[37] However, direct immune modulation may have adverse effects, whereas targeting inflammation by regulating the gut microbiota could offer a more favorable risk profile.[38] Th17 and Treg cells are two important CD4+ T cell subsets involved in immune regulation, and their imbalance is closely tied to many immune diseases. There are studies showing that ovariectomy expanded intestinal Th17 cells and TNF+ T cells, increased their S1P receptor 1–mediated egress from the intestine, and enhanced their subsequent influx into the bone marrow through CXCR3- and CCL20-mediated mechanisms. Therefore, blockade of Th17 cell and TNF+ T cell egress from the gut or their influx into the bone marrow prevented bone loss associated with sex steroid deficiency.[11,39] Furthermore, Immune system interactions with gut microbiota also affect bone health, a large number of studies have emphasized the importance of gut microbiota to support intestinal immunity by balancing Th17 and Treg cells. Probiotics can enhance the function of the intestinal barrier by increasing the expression levels of genes involved in tight junction formation, thereby reducing the invasion of intestinal pathogens and harmful products into the host and reducing the inflammation-induced immune response.[40] Our findings suggest that QEP regulates Th17/Treg balance in the gut-bone axis, thereby improving immune status. This effect may be through direct enhancement of the abundance of *Lactobacillus* (demonstrated both in vivo and in vitro) and alterations of fecal metabolic profile. Although the in vitro results showed some differences from the in vivo findings, which may be attributed to the effects of the anaerobic condition and intestinal environment of the host, *Lactobacillus* was the dominant species in both experimental settings. Several studies have consistently demonstrated the beneficial effects of *Lactobacillus* on osteoporosis.[19,41] One of our previous studies also showed that *Lactobacillus rhamnosus* GG can directly modulate Th17/Treg balance in the gut-bone axis.[19] It is noteworthy that *Lactobacillus* can ameliorate intestinal barrier damage in rat by producing SCFA indole

derivatives and polyamines.[42] Many studies have demonstrated that gut microbiota and their associated metabolites can modulate host bone metabolism by influencing host metabolism and immunity. Our study revealed that QEP significantly altered the metabolic profile of OVX rats, with these alterations being significantly correlated with changes in the gut microbiota, particularly *Lactobacillus*.

Nevertheless, our study has certain limitations: 1) different species within the same genus may exhibit distinct therapeutic effects and mechanisms of action.[43] Therefore, the application of metagenomics to explore the composition and dynamics of intestinal flora in OVX models, identify additional potential probiotic species, and conduct relevant studies remain an imperative future endeavor. 2) Targeted metabolomics require further validation for identifying potential biomarkers. 3) Lack of human clinical data. The species-specific disparities in gut microbiota profiles (*Lactobacillus* dominance variations) and immune regulation pathways (Th17/Treg balance) between rats and human may limit the applicability of the findings. Future clinical trials should be explored QEP's effects on gut microbiota composition and long-term safety and elucidate QEP's immunomodulatory pathway in postmenopausal women. In summary, these results provided a solid foundation for further research and development of QEP, while illuminating the mechanisms through which traditional Chinese medicine effectively combated PMOP.

Conclusion

In conclusion, this study demonstrated that QEP can effectively ameliorate osteoporosis by regulating the Th17/Treg balance and enriching the gut microbes in OVX rats. Correlation analysis revealed significant associations among *Lactobacillus* and Th17/Treg-related factors. Of note, the bacteria of *Lactobacillus* and *Bacteroides* may be beneficial to regulate Th17/Treg balance in gut-bone axis. Furthermore, QEP significantly altered the metabonomic profile including estrone metabolism, steroidogenesis, androgen and estrogen metabolism, androstenedione metabolism and alpha linolenic acid and linoleic acid metabolism. These findings suggest that QEP may serve as a safe and effective alternative therapy for PMOP, establishing both a robust theoretical foundation and empirical support for its clinical application. To ensure the efficacy and safety of QEP in clinical long-term use, further clinical trials are warranted in humans. Moreover, potential functional probiotics and prebiotics associated with *Lactobacillus* and QEP will also be further studied in the future.

Abbreviations

ALA, alpha-linolenic acid; BM, bone marrow; BMD, bone mineral density; BV/TV, bone volume fraction; CTX-I, C-telopeptide of type I collagen; IL-17, interleukin 17; MLN, mesenteric lymph nodes; OVX, ovariectomized; PINP, procollagen type I N-terminal propeptide; QEP, Qing'e pills; SMI, structure model index; Tb.N, trabecular number; Tb.Th, trabecular thickness; Tb.Sp, trabecular separation; TGF-β, transforming growth factor-beta; TNF-α, tumor necrosis factor-alpha.

Ethics Approval

Animal experiments were conducted in compliance with the Guide for the Care and Use of Laboratory Animals published by the National Institutes of Health and were approved by the Animal Ethics Committee of the Nanjing University of Traditional Chinese Medicine (approval number: 202109A025).

Author Contributions

All authors contributed to data analysis, drafting or revising the article, gave final approval of the version to be published; have agreed on the journal to which the article has been submitted; and agree to be accountable for all aspects of the work.

Funding

This work was financially supported by the National Natural Science Foundation of China (Grant numbers 81973484, 81773902, and 82204621).

Disclosure

The authors declare that there are no conflicts of interest.

References

1. Adami G, Fassio A, Gatti D, et al. Osteoporosis in 10 years time: a glimpse into the future of osteoporosis. *Ther Adv Musculoskelet Dis*. 2022;14:1759720x221083541. doi:10.1177/1759720x221083541
2. Ensrud KE, Crandall CJ. Osteoporosis. *Ann Intern Med*. 2024;177(1):Itc1–itc16. doi:10.7326/aitc202401160
3. Jia L, Tu Y, Jia X, et al. Probiotics ameliorate alveolar bone loss by regulating gut microbiota. *Cell Proliferation*. 2021;54(7):e13075. doi:10.1111/cpr.13075
4. Zhang JY, Zhong YH, Chen LM, Zhuo XL, Zhao LJ, Wang YT. Recent advance of small-molecule drugs for clinical treatment of osteoporosis: a review. *Eur J Med Chem*. 2023;259:115654. doi:10.1016/j.ejmech.2023.115654
5. Janovská Z. Bisphosphonate-related osteonecrosis of the jaws. A severe side effect of bisphosphonate therapy. *Acta medica*. 2012;55(3):111–115. doi:10.14712/18059694.2015.47
6. Elbers LPB, Raterman HG, Lems WF. Bone mineral density loss and fracture risk after discontinuation of anti-osteoporotic drug treatment: a narrative review. *Drugs*. 2021;81(14):1645–1655. doi:10.1007/s40265-021-01587-x
7. Pan M, Pan X, Zhou J, Wang J, Qi Q, Wang L. Update on hormone therapy for the management of postmenopausal women. *Biosci Trends*. 2022;16(1):46–57. doi:10.5582/bst.2021.01418
8. Li JY, Chassaing B, Tyagi AM, et al. Sex steroid deficiency-associated bone loss is microbiota dependent and prevented by probiotics. *J Clin Invest*. 2016;126(6):2049–2063. doi:10.1172/jci86062
9. Yang X, Zhou F, Yuan P, et al. T cell-depleting nanoparticles ameliorate bone loss by reducing activated T cells and regulating the Treg/Th17 balance. *Bioact Mater*. 2021;6(10):3150–3163. doi:10.1016/j.bioactmat.2021.02.034
10. Gao P, Pan X, Wang S, et al. Identification of the transcriptome signatures and immune-inflammatory responses in postmenopausal osteoporosis. *Heliyon*. 2024;10(1):e23675. doi:10.1016/j.heliyon.2023.e23675
11. Yu M, Pal S, Paterson CW, et al. Ovariectomy induces bone loss via microbial-dependent trafficking of intestinal TNF+ T cells and Th17 cells. *J Clin Invest*. 2021;131(4). doi:10.1172/jci143137
12. Ni JJ, Yang XL, Zhang H, et al. Assessing causal relationship from gut microbiota to heel bone mineral density. *Bone*. 2021;143:115652. doi:10.1016/j.bone.2020.115652
13. Zhou T, Wang M, Ma H, Li X, Heianza Y, Qi L. Dietary fiber, genetic variations of gut microbiota-derived short-chain fatty acids, and bone health in UK biobank. *J Clin Endocrinol Metab*. 2021;106(1):201–210. doi:10.1210/clinem/dgaa740
14. Hao J, Bei J, Li Z, et al. Qing`e pill inhibits osteoblast ferroptosis via ATM serine/threonine kinase (ATM) and the PI3K/AKT pathway in primary osteoporosis. *Front Pharmacol*. 2022;13:902102. doi:10.3389/fphar.2022.902102
15. Li J, Guo X. Chronic toxicity of Qing ‘e pills in normal rats. *Chin J Pharmacovigilance*. 2021;18(05):444–453. in Chinese.
16. Xin G, Taotao C, Huang N, Rong S. Experimental study on acute toxicity of Qing ‘e pills and their separated prescriptions aqueous extract in normal mice. *Chin J Pharmacovigilance*. 2021;18(5):427–432. in Chinese.
17. Xiong JL, Cai XY, Zhang ZJ, Li Q, Zhou Q, Wang ZT. Elucidating the estrogen-like effects and biocompatibility of the herbal components in the Qing’ E formula. *J Ethnopharmacol*. 2022;283:114735. doi:10.1016/j.jep.2021.114735
18. Xie H, Hua Z, Guo M, et al. Gut microbiota and metabonomics used to explore the mechanism of Qing’e pills in alleviating osteoporosis. *Pharm Biol*. 2022;60(1):785–800. doi:10.1080/13880209.2022.2056208
19. Guo M, Liu H, Yu Y, et al. Lactobacillus rhamnosus GG ameliorates osteoporosis in ovariectomized rats by regulating the Th17/Treg balance and gut microbiota structure. *Gut Microbes*. 2023;15(1):2190304. doi:10.1080/19490976.2023.2190304
20. Zhang J, Liang X, Tian X, et al. Bifidobacterium improves oestrogen-deficiency-induced osteoporosis in mice by modulating intestinal immunity. *Food Funct*. 2024;15(4):1840–1851. doi:10.1039/d3fo05212e
21. Foessl I, Dimai HP, Obermayer-Pietsch B. Long-term and sequential treatment for osteoporosis. *Nat Rev Endocrinol*. 2023;19(9):520–533. doi:10.1038/s41574-023-00866-9
22. Skjødt MK, Frost M, Abrahamsen B. Side effects of drugs for osteoporosis and metastatic bone disease. *Br J Clin Pharmacol*. 2019;85(6):1063–1071. doi:10.1111/bcp.13759
23. Pacifici R. Bone remodeling and the microbiome. *Cold Spring Harb Perspect Med*. 2018;8(4):a031203. doi:10.1101/cshperspect.a031203
24. Xu Q, Li D, Chen J, et al. Crosstalk between the gut microbiota and postmenopausal osteoporosis: mechanisms and applications. *Int Immunopharmacol*. 2022;110:108998. doi:10.1016/j.intimp.2022.108998
25. Xu L, Sun X, Han X, et al. Dihydromyricetin ameliorate postmenopausal osteoporosis in ovariectomized mice: integrative microbiomic and metabolomic analysis. *Front Pharmacol*. 2024;15:1452921. doi:10.3389/fphar.2024.1452921
26. Wang S, Wang S, Wang X. Effects of icariin on modulating gut microbiota and regulating metabolite alterations to prevent bone loss in ovariectomized rat model. *Front Endocrinol*. 2022;13:874849. doi:10.3389/fendo.2022.874849
27. Jiang T, Li C, Li Y, et al. Multi-omics and bioinformatics for the investigation of therapeutic mechanism of roucongrong pill against postmenopausal osteoporosis. *J Ethnopharmacol*. 2025;337(Pt 2):118873. doi:10.1016/j.jep.2024.118873
28. Chen C, Cao Z, Lei H, et al. Microbial tryptophan metabolites ameliorate ovariectomy-induced bone loss by repairing intestinal ahr-mediated gut-bone signaling pathway. *Adv Sci*. 2024;11(36):e2404545. doi:10.1002/advs.202404545
29. Hayes D, Angove MJ, Tucci J, Dennis C. Walnuts (Juglans regia) chemical composition and research in human health. *Crit Rev Food Sci Nutr*. 2016;56(8):1231–1241. doi:10.1080/10408398.2012.760516
30. Holscher HD. Gut microbes: nuts about fatty acids. *J Nutr*. 2020;150(4):652–653. doi:10.1093/jn/nxaa045
31. Miyamoto J, Igarashi M, Watanabe K, et al. Gut microbiota confers host resistance to obesity by metabolizing dietary polyunsaturated fatty acids. *Nat Commun*. 2019;10(1):4007. doi:10.1038/s41467-019-11978-0
32. Watson H, Mitra S, Croden FC, et al. A randomised trial of the effect of omega-3 polyunsaturated fatty acid supplements on the human intestinal microbiota. *Gut*. 2018;67(11):1974–1983. doi:10.1136/gutjnl-2017-314968

33. Loo YT, Howell K, Chan M, Zhang P, Ng K. Modulation of the human gut microbiota by phenolics and phenolic fiber-rich foods. *Compr Rev Food Sci Food Saf*. 2020;19(4):1268–1298. doi:10.1111/1541-4337.12563
34. Song J, Zhang Y, Zhu Y, et al. Structural characterization and anti-osteoporosis effects of polysaccharide purified from Eucommia ulmoides Oliver cortex based on its modulation on bone metabolism. *Carbohydr Polym*. 2023;306:120601. doi:10.1016/j.carbpol.2023.120601
35. Yuan S, Shen J. Bacteroides vulgatus diminishes colonic microbiota dysbiosis ameliorating lumbar bone loss in ovariectomized mice. *Bone*. 2021;142:115710. doi:10.1016/j.bone.2020.115710
36. Brown EM, Ke X, Hitchcock D, et al. Bacteroides-derived sphingolipids are critical for maintaining intestinal homeostasis and symbiosis. *Cell Host Microbe*. 2019;25(5):668–680.e7. doi:10.1016/j.chom.2019.04.002
37. Fischer V, Haffner-Luntzer M. Interaction between bone and immune cells: implications for postmenopausal osteoporosis. *Semin Cell Dev Biol*. 2022;123:14–21. doi:10.1016/j.semcdb.2021.05.014
38. Rizzoli R, Biver E. Are probiotics the new calcium and vitamin D for bone health? *Curr Osteoporos Rep*. 2020;18(3):273–284. doi:10.1007/s11914-020-00591-6
39. Lorenzo J. From the gut to bone: connecting the gut microbiota with Th17 T lymphocytes and postmenopausal osteoporosis. *J Clin Invest*. 2021;131(5). doi:10.1172/jci146619
40. Wang J, Hou Y, Mu L, Yang M, Ai X. Gut microbiota contributes to the intestinal and extraintestinal immune homeostasis by balancing Th17/Treg cells. *Int Immunopharmacol*. 2024;143(Pt 3):113570. doi:10.1016/j.intimp.2024.113570
41. Lee CS, Kim SH. Anti-inflammatory and anti-osteoporotic potential of Lactobacillus plantarum A41 and L. fermentum SRK414 as probiotics. *Probiotics Antimicrob Proteins*. 2020;12(2):623–634. doi:10.1007/s12602-019-09577-y
42. Wang A, Guan C, Wang T, Mu G, Tuo Y. Lactobacillus-derived indole derivatives ameliorate intestinal barrier damage in rat pups with complementary food administration. *Food Funct*. 2024;15(17):8775–8787. doi:10.1039/d4fo02230k
43. Wang C, Xiao Y, Yu L, et al. Protective effects of different Bacteroides vulgatus strains against lipopolysaccharide-induced acute intestinal injury, and their underlying functional genes. *J Adv Res*. 2022;36:27–37. doi:10.1016/j.jare.2021.06.012